HHS Public Access

Author manuscript

Dev Biol. Author manuscript; available in PMC 2018 February 15.

Published in final edited form as:

Dev Biol. 2017 February 15; 422(2): 171–185. doi:10.1016/j.ydbio.2016.12.013.

Inactivation of maternal *Hif-1α* at mid-pregnancy causes placental defects and deficits in oxygen delivery to the fetal organs under hypoxic stress

Doreswamy Kenchegowda[a], **Bryony Natale**[c], **Maria Lemus**[c], **David R. Natale**[c,*], and **Steven A. Fisher**[a,b,*]

[a]Department of Cardiovascular Medicine, University of Maryland School of Medicine, Baltimore, MD 21201

[b]Department of Physiology, University of Maryland School of Medicine, Baltimore, MD 21201

[c]Department of Reproductive Medicine, University of California San Diego, La Jolla, CA 92093

Abstract

A critical transition occurs near mid-gestation of mammalian pregnancy. Prior to this transition, low concentrations of oxygen (hypoxia) signaling through Hypoxia Inducible Factor (HIF) functions as a morphogen for the placenta and fetal organs. Subsequently, functional coupling of the placenta and fetal cardiovascular system for oxygen (O_2) transport is required to support the continued growth and development of the fetus. Here we tested the hypothesis that *Hif-1α* is required in maternal cells for placental morphogenesis and function. We used Tamoxifen-inducible Cre-Lox to inactivate *Hif-1α* in maternal tissues at E8.5 (MATcKO), and used ODD-Luciferase as a reporter of hypoxia in placenta and fetal tissues. MATcKO of *Hif-1α* reduced the number of uterine natural killer (uNK) cells and *Tpbpa*-positve trophoblast cells in the maternal decidua at E13.5 −15.5. There were dynamic changes in all three layers of E13.5–15.5 MATcKO placenta. Of note was the under-development of the labyrinth at E15.5 associated with reduced Ki67 and increased TUNEL staining consistent with reduced cell proliferation and increased apoptosis. Labyrinth defects were particularly evident in placentas connected to effectively *HIF-1α* heterozygous null embryos. MATcKO had no effect on basal ODD-Luciferase activity in fetal organs (heart, liver, brain) at any stage, but at E13.5 −15.5 resulted in enhanced induction of the ODD-Luciferase hypoxia reporter when the dam's inspired O_2 was reduced to 8% for 4 hours. MATcKO also slowed the growth after E13.5 of fetuses that were effectively heterozygous for *Hif-1α*, with most being non-viable at E15.5. The hearts of these E15.5 fetuses were abnormal with reduction in size, thickened epicardium and mesenchymal septum. We conclude that maternal HIF-1α is required for placentation, specifically, recruitment of uNK and trophoblast cells into the

[*]**Corresponding authors:** Steven A. Fisher, MD, 20 Penn Street, HSF2, Room- S012C, Baltimore MD 21201, Phone: 410-706-4534, Fax: 410-706-0670, SFisher1@medicine.umaryland.edu. David R. Natale, PhD, 2A03 Leichtag Biomedical Research Building, 9500 Gilman Drive, MC 0674, La Jolla CA 92093-0674, Phone: 858-822-0758, Fax: 858-534-1438, dnatale@ucsd.edu.

maternal decidua and other trophoblast cell behaviors. The placental defects render the fetus vulnerable to O_2 deprivation after mid-gestation.

Keywords

trophoblast; feto-placental unit; uterine natural killer cells

1. INTRODUCTION

During mammalian pregnancy the delivery of O_2 and nutrients to the developing embryo must increase in order for it to grow in size and complexity (reviewed in (Bishop and Ratcliffe, 2015; Fisher and Burggren, 2007). These metabolic needs are met by the formation of the placenta, so that O_2, nutrients and waste can be exchanged between the mother and fetus, and the development of a functional fetal cardiovascular system for the distribution of O_2 and nutrients to, and removal of wastes from the growing organs. Functional maturation of the feto-placental unit (FPU) and resultant increase in O_2 supply occurs near mid-gestation in the mouse and rat (E11–14) and towards the end of the 1st trimester in humans (8–12 weeks) (Jauniaux et al., 2003; Murray, 2012). Prior to FPU maturation the relative lack of O_2 (tissue hypoxia), which leads to signaling through the HIF, is thought to be a morphogen for organs that are subsequently required for O_2 delivery, including the placenta, blood, heart and vascular system (reviewed in (Dunwoodie, 2009). Consistent with this paradigm, germline inactivation of HIF subunits results in non-viable embryos by mid-gestation (~E10.5 in mouse) with structural defects in each of these organ systems (reviewed in (Dunwoodie, 2009).

Defining a specific role for O_2-sensing and HIF in each of these organs is confounded by the interdependence of the fetal organs and placenta for O_2 delivery and development, as well as the pleiotropic effects of vascular insufficiency and tissue hypoxia on morphogenesis, organ function and survival. To circumvent these limitations, conditional approaches have been used to inactivate *Hif* genes in specific cell types or at specific stages of development (reviewed in (Bishop and Ratcliffe, 2015)). In a prior study, we showed that Tamoxifen-inducible *Cre*-mediated cKO of *Hif-1α* at E9.5 caused defects in the formation of the structures of the cardiac outflow tract, modeling human congenital heart defects (CHD) (Kenchegowda et al., 2014). However, the Tamoxifen-inducible *Cre* was under the control of the pan-active *β-actin* promoter, raising the possibility that inactivation of *Hif* in other organs, in particular the placenta, could contribute to the formation of the structural heart defects. This line of reasoning is supported by several observations: 1) many gene KOs in the mouse cause fetal and placental defects (reviewed in (Watson and Cross, 2005) 2) Hypoxia signaling through HIF has been proposed to play a number of roles in placental development, including migration and differentiation of cells in all three layers of the placenta (reviewed in (Burton, 2009; Maltepe et al., 2010; Pringle et al., 2010; Soares et al., 2014) and 3) in both rodents and more recently, in humans, an association between placental and fetal heart defects has been described (Adams et al., 2000; Auger et al., 2015; Barak et al., 1999; Brodwall et al., 2016; Llurba et al., 2014; Sliwa and Mebazaa, 2014). However, the extent to which placental dysmorphogenesis and resultant dysfunction may compromise

O_2 delivery to the organs of a growing and viable fetus is not clear, particularly in mouse models. Study of the *Rag2*$^{-/-}$*Il2rg*$^{-/-}$ (Recombination activating gene 2, Interleukin 2 receptor, gamma) double KO (lymphocyte/NK cell-deficient) mouse model (Ashkar et al., 2000) suggested that placental defects had no effect on O_2 delivery (Leno-Duran et al., 2010).

Studies in the rat suggest that 1) hypoxia in the maternal compartment activates endovascular trophoblast invasion and uterine vascular remodeling (Rosario et al., 2008) and 2) maternally-derived uNK cells invade the maternal decidua and regulate trophoblast behaviors in a hypoxia-sensitive manner (Chakraborty et al., 2011). The goals of the current study were 1) to test the role of hypoxia signaling through HIF in the maternal cells in placentation and 2) to determine how this alteration of HIF signaling affects the placenta's ability to deliver O_2 to the organs of the growing fetus. To achieve the former, we used a Tamoxifen-inducible *β-actinCre* to inactivate *Hif-1α* in the maternal cells at specific gestational stages. For the latter, the mice expressed the ODD-Luc hypoxia reporter which contains the Oxygen Degradation Domain (ODD) of *Hif-1α* fused to the N-terminus of the Luciferase (Luc) coding sequence constitutively expressed from the ROSA26 locus (ODD-Luc) (Safran et al., 2006).

2. METHODS

2.1. Mice

Mice were handled in accordance with University of Maryland Baltimore Institutional Animal Care and Use Committee guidelines. All mouse strains used in this study were obtained from Jackson Laboratory and maintained as a breeding colony at University of Maryland-Baltimore. ODD-Luc mice (Safran et al., 2006) (stock # 006206) were maintained as homozygotes in an FVB background. ODD-Luc males and females were mated and tissues harvested from E9.5 to maturity for measurement of ODDLuc activity as described below. Tamoxifen (TM) inducible *β-actinCre*$^{+}$ (*CAGGCre-ER™*; stock # 004682) (Hayashi and McMahon, 2002) mice were crossed with *Hif-1α*$^{f/f}$ mice in which LoxP sites flank exon 2 of *Hif-1α* (stock # 007561) (Ryan et al., 2000) to obtain *Hif-1α*$^{f/f}$,*β-actinCre*$^{+}$ females. For maternal conditional inactivation of *Hif-1α* (MATcKO), timed matings were performed with *Hif-1α*$^{f/f}$,*β-actinCre*$^{+}$ females and ODD-Luc males (*Hif-1α*$^{+/+}$) with the presence of a vaginal plug in the morning counted as E0.5. Pregnant dams were treated with TM (3mg/40g bw; Sigma # T5648) in sunflower oil on E8.5 and 9.5 to induce the activity of Cre recombinase as previously described (Hayashi and McMahon, 2002; Kenchegowda et al., 2014). Mice were genotyped by standard PCR methods using primers as described on the Jackson Laboratory website. PCR of genomic DNA was performed to test Cre efficiency using forward 5' GGATGAAAACATCTGCTTTGG 3' and reverse 5' ACTGCCCCAACACAATACTTTT 3' primers. Recombination of *Hif-1α was* ~90% in the MATcKO placentas of Tamoxifen-treated mice measured at E15.5 vs <20% in placentas of untreated (control) mice of the same genotype.

2.2. Maternal exposures to hypoxia

Timed pregnant mice (MATcKO, ODD-Luc) were placed in modular incubator chambers (Billups-Rothenberg Inc.) on E11.5, 13.5 or 15.5. The chamber was flushed with gas from a tank containing 8% O_2/ 92% nitrogen (Airgas) and then clamped. The mice were maintained in this chamber for 4 hours with free access to food and water and tolerated this procedure well. For control experiments, pregnant dams were placed in the chamber and flushed with gas from a tank containing 21 % O_2 / 79% nitrogen (room air), for 4 hours with free access to food and water.

2.3. Measurement of luciferase activity

Pregnant dams were euthanized by CO_2 inhalation followed by cervical dislocation and the uterine horns removed and placed in ice-cold PBS. Placenta and embryonic tissues were dissected under a stereomicroscope in ice cold PBS and stored at −80°C. Tissues were homogenized in 1X Cell Culture Lysis Reagent (Promega) and clarified by centrifugation. 10–20μl of the lysate was transferred to a 96 well plate and firefly luciferase activity measured as per manufacturer's instructions (Promega) using a microplate reader (Flex Station 3, Molecular Devices) as previously described (Kenchegowda et al., 2014). Protein concentrations in the lysate were measured using the Bio-Rad Protein Assay Dye Reagent with BSA as the protein standard. Luminescence Units (LU) were normalized to total protein and expressed as femtomoles of luciferase /mg protein using QuantiLum Recombinant Luciferase (Promega) as the standard.

2.4. Analysis of placental morphology and histology

Pregnant dams were euthanized by CO_2 inhalation on E13.5 and E15.5. Placentas and embryos were dissected and fixed in formalin (10% w/v) in PBS overnight at 4°C. Fixed embryos were washed with PBS and stored in 70% ethanol at 4°C. Whole mount images of placenta and embryos were captured using Leica MZFLIII stereomicroscope (Leica). For the preparation of paraffin blocks, tissues were dehydrated through a graded series of ethanol and xylene and embedded in paraffin wax. Sections 6 μm in thickness were deparaffinized and rehydrated through a series of ethanol and subjected to Hematoxylin and Eosin stain according to standard protocols as previously described (Natale et al., 2006). In all of the experiments, representative sections from the center of the placenta were analyzed. Images were captured using EVOS XL Core (Life Technologies) and Leica DMLB (Leica) microscopes and Spot RT3 camera (Diagnostic Instruments).

RNA *in situ* hybridization was conducted on 6 μm paraffin sections as previously described (Hughes et al., 2013; Natale et al., 2009; Simmons et al., 2008a). Riboprobes for trophoblast markers *Gcm1*, *Plp-f* (*Prl7a2*), *Plp-n* (*Prl7b1*), *Pcdh12*, *Syna*, *Tpbpa* and *Plf* (*Prl2c2*) were synthesized as previously described (Hughes et al., 2013; Natale et al., 2009; Simmons et al., 2008b). Immunostaining was performed to detect Ki67 and Perforin as markers of cell proliferation and uNK cells, respectively. Sections were deparaffinized and rehydrated followed by antigen retrieval in Citrate buffer (Biogenex) using a 2100-Retriever (Electron Microscopy Science). Sections were treated with 3% H_2O_2 to quench endogenous peroxidase, washed in PBS and blocked with 5% goat serum, 0.1% BSA in PBS for 1 hour at room temperature. Sections were incubated with anti-Ki67 (ab16667) or anti-Perforin

(ab16074) primary antibodies (Abcam) at 1:300 at room temperature for 1 hour. The remainder of the procedure followed the manufacturer's protocol using ImmPRESS HRP Anti-Rabbit polymer detection kit (Vector Laboratories). Antibody binding was detected using DAB system according to the manufacturer's protocol (Vector Laboratories). Following counterstaining in hematoxylin (Gills #2, Sigma-Aldrich) or Nuclear Fast Red (Vector Laboratories), sections were dehydrated and mounted in xylene-based mounting medium.

Alkaline phosphatase (AP) staining to identify maternal blood spaces was conducted as previously described (Natale et al., 2006). Periodic Acid Schiff (PAS) staining to identify glycogen accumulation was conducted according to the manufacturer's protocol (Sigma-Aldrich). TUNEL staining to detect cells undergoing apoptosis was carried out using the *in situ* Cell Death Detection kit from Roche (Sigma-Aldrich) according to the manufacturer's protocol.

Semi-quantitative assessment of placental layers and *in situ* hybridization staining in placenta sections was conducted using NIH ImageJ software. Regions of staining were outlined and measured using ImageJ. Area was calculated as a proportion of the total measured area of each of the placentas and reported as % area. At least three independent placentas were measured for each gene or layer quantified.

2.5. Statistical Analysis

Data are expressed as mean ± SEM. Multiple groups were compared by One-Way ANOVA with Bonferroni correction using SigmaPlot 12 (Systat Software). Differences between paired groups were examined by Student's unpaired t-test. $P<0.05$ was considered statistically significant.

3. RESULTS

3.1. Effect of MATcKO on fetal and placental development and morphology

Timed pregnant mice of the genotype *Hif-1α*$^{f/f}$,*β-actinCre*$^{+}$ were treated with TM at E8.5 and 9.5 unless noted otherwise. These mice will hereafter be designated as MATcKO. The mice were examined at E13.5 and E15.5 when placental and fetal organ morphogenesis are nearing completion. It is important to note that following TM treatment, the dams and any maternally-derived components of the placenta were effectively homozygous null for *Hif-1α*, however, the resulting embryo and fetal-derived contribution to the placenta were either effectively heterozygous for the *Hif*-1α null allele (50% *HIF-1α* $^{f/+}$,*β-actinCre*$^{+}$) or functionally wild type (50%; *HIF-1αf*$^{/+}$,*β-actinCre*). Timed pregnant mice of genotype *Hif-1α*$^{+/+}$,*β-actinCre*$^{+}$ treated similarly with TM served as controls (CON).

MATcKO placentas were analyzed according to the genotype of the embryo. *HIF-1α* $^{f/+}$,*β-actinCre*$^{+}$ embryo are designated E:Cre+ and *HIF-1α* $^{f/+}$,*β-actinCre*$^{-}$ embryo as E:Cre−. MATcKO placentas associated with E:Cre+ and E:Cre− embryos are designated as MATcKO E:Cre^{-}, respectively. When there was no difference between placentas supplying Cre^{+} vs Cre^{-} embryos, the sub-groups are lumped together and described as MATcKO. There were no differences in placental size and weight at E13.5 (data not shown). At E15.5

MATcKO E:Cre^{+} placentas were visibly smaller and weighed ~15% less than CON while MATcKO E:Cre^{-} placentas were unchanged (CON: 98.1±2.0mg; MATcKO E:Cre^{+}: 84.4±1.5mg, P<0.001; MATcKO E:Cre^{-}: 104.7±2.83mg, p=0.08). The general appearance of MATcKO placentas was normal while a number of abnormalities were evident in histological assays. In E13.5 CON the decidua comprised ~50% of the placenta area, while in the MATcKO placentas this was reduced to ~35% with a corresponding increase in the junctional zone (Table 1, Fig. 1). At E15.5 the decidua was relatively reduced to comprise ~25% of CON placenta, with corresponding and relatively equal increases in junctional and labyrinth zones, consistent with prior studies (Natale et al., 2006). MATcKO E:Cre^{-} placentas displayed a similar developmental trend as CON such that at E15.5 there were no differences between these groups in the relative contributions of the different layers. In contrast in MATcKO E:Cre^{+} placentas the relative proportions of the decidual, junctional and labyrinth zones did not change from E13.5 to E15.5. Thus, the relative contribution of decidua was higher in MATcKO E:Cre^{+} E15.5 placentas as compared to the other groups.

3.2. Trophoblast Differentiation

Tpbpa, *Plp-F* (*Prl7a2*), *Plp-N* (*Prl7b1*), *Plf* (*Prl2c2*), *Gcm1* and *Syna* mRNAs were used as markers of trophoblast differentiation and detected by *in situ* hybridization. *Tpbpa* is a marker of spongiotrophoblasts (Sp-T) and glycogen trophoblasts (Gly-T), *Plp-F* marks Sp-T only, and *Plp-N* identifies Gly-T cells in all junctional zone subtypes (Simmons et al., 2008b). The expression of *Tpbpa* at E13.5, as a proportion of the total area of the placenta, was significantly increased in MATcKO placentas compared to CON, regardless of fetal genotype (Table 2, Fig. 1 E , F). At E15.5, the proportional area of *Tpbpa* expression in the CON placentas had increased and was now equal to that of E15.5 MATcKO placentas, in which proportions had not changed from E13.5 (Fig. 1, G, H). *Plp-F* and *Plp-N*, markers of spongiotrophoblasts and glycogen trophoblasts, respectively, showed staining patterns concordant in the junctional zone consistent with *Tpbpa* staining. These markers were increased in E13.5 MATcKO placentas but similar to CON in E15.5 MATcKO placentas (Table 2, Fig. 2A–H). Of note, many Gly-T appeared earlier in the decidua of MATcKO placentas (E13.5) vs CON. At higher magnification the Gly-T, identified by PAS staining and their large, vacuolated morphology (Fig. 2I, J, arrows), appeared smaller in the junctional zone of E15.5 MATcKO placentas.

Plf (*Prl2c2*) identifies parietal trophoblast giant cells (p-TGCs) located at the border of the fetal placenta and decidua, and spiral artery trophoblast giant cells (SA-TGCs) associated with spiral arteries (SA) in the maternal decidua, where they participate in arterial remodeling (Adamson et al., 2002; Hemberger et al., 2003; Simmons and Cross, 2005; Simmons et al., 2008a). *Plf* (*Prl2c2*)-positive trophoblast cells were observed in E13.5 (not shown) and E15.5 (Fig. 3A, B) CON and MATcKO placentas at the border of the maternal decidua and fetal placenta (not shown). At higher magnification, the association of SA-TGCs with maternal decidua SAs appeared to be reduced in the MATcKO placentas (Fig. 3C, D, arrows). Furthermore, *Plf* (*Prl2c2*) staining appeared to be more frequent in the labyrinth layer of MATcKO placentas (Fig. 3A, B, arrows), suggesting aberrant TGC differentiation and/or migration into the labyrinth zone in the placentas of these mice.

Syna and *Gcm1* were used as markers of syncytiotrophoblasts (Syn-T) of layers I and II of the labyrinth zone, respectively. *Syna*- and *Gcm1*-positive cells appeared reduced in number in the labyrinth layer of E13.5 and E15.5 MATcKO placentas (*Gcm1*, Fig. 4A–H; *Syna* data not shown). In E13.5 and 15.5 CON placentas, *Gcm1* staining was evenly distributed throughout the labyrinth layer and associated with blood spaces. In MATcKO placentas, *Gcm1* positive cells were smaller and less frequent. Beginning at E13.5 and by E15.5, they were very obviously reduced and not all were associated with blood spaces. This suggests underdevelopment of the labyrinth layer in MATcKO placentas. To complete this assessment, alkaline phosphatase (AP) staining was used to identify sinusoidal trophoblast giant cells (S-TGCs) surrounding maternal blood spaces within the labyrinth and thus provide an indication of overall maternal vascular development. AP staining in CON and MATcKO placentas at E13.5 was similar and showed cellular, avascular regions as well as clearly defined maternal blood spaces (not shown). Clusters of undifferentiated cells in the labyrinth layer are common in the normal formation of the placenta as it develops and expands from E9.5 to E14.5. In MATcKO E15.5 placentas, regions devoid of alkaline phosphatase staining persisted and were more numerous in the labyrinth layer as compared to CON (Fig. 4I, J, dotted lines). At higher magnification, it was evident that these regions were cellular, avascular and resembled the Sp-T and Gly-T cells of the junctional zone (Fig. 4I, J, arrows in insets) rather than undifferentiated cells. *Tpbpa* positive staining throughout the labyrinth suggests these regions represent mislocalized junctional zone trophoblast cell subtypes (see Fig. 1, compare E & F).

3.3. Uterine Natural Killer (uNK) cells

uNK cells were identified by Perforin (Prf) immunostaining. These maternally derived immune cells are recruited to the maternal decidua, and thought to play a role in the remodeling of the SAs (Chakraborty et al., 2011; Tessier et al., 2015). As expected Prf-positive uNK cells were abundant in E13.5 CON decidua and had significantly declined by E15.5 (Fig. 5). At higher magnification, these cells could be seen encircling vessels within the decidua (Fig. 5G, arrows). Prf- positive uNK cells were present in the decidua of E13.5 and E15.5 MATcKO but significantly decreased as compared to gestational age-matched CON (Fig. 5). At higher magnification the uNK cells in the decidua of MATcKO did not appear to localize to any particular anatomic structure (Fig. 5H).

3.4. Proliferation and Apoptosis in the Placenta

Placentas were stained for Ki67 and TUNEL to determine if the atrophy of MATcKO E:Cre$^+$ placentas may be due to reduced cell proliferation and/or increased cell death (apoptosis), respectively. As expected Ki67 positive cells were restricted to the labyrinth of all E15.5 placentas, however they were significantly reduced in the MATcKO E:Cre$^+$ (Fig. 6A–E, arrows in C, D). In contrast, TUNEL positive cells were increased in the labyrinth of E15.5 MATcKO E:Cre$^+$ placentas (Fig. 7A–D, arrows in D). Together this suggests decreased proliferation and increased apoptosis specifically in the labyrinth layer of E15.5 MATcKO E:Cre$^+$ placentas.

3.5. ODD-Luc activity as a reporter of tissue O_2 during normal development

The structural defects observed in the placenta could result in placental dysfunction. To test this, ODD-Luc was used as a surrogate indicator of the sufficiency of O_2 transport to the fetal tissues. Luciferase activity was measured in lysates of placenta and fetal organs of timed pregnant mice. Males and females in this mating were homozygous for ODD-Luc at the ROSA26 locus and otherwise wild-type. Some of the data on ODD-Luc activity in fetal organs was previously published (Kenchegowda et al., 2014). ODD-Luc activity was 2–10 fold lower in the placenta as compared to the fetal organs dependent upon the gestational age and organ (Fig. 8A–D). Placental ODD-Luc activity declined during development from a high at E9.5 to a level that was approximately one-third of that at E17.5. The developmental decline in placental ODD-Luc activity was shallower than that of the fetal organs and with a distinct timing. Whereas fetal heart, liver and brain all had ~2–4 fold declines in ODD-Luc activity from E10.5–13.5, the placenta had a more gradual decline with the largest change occurring from E13.5–17.5. In each fetal organ ODD-Luc activity declined from E10.5–13.5 with further declines around the time of birth (E17.5- PN5) and from PN5 to full maturity at 8 weeks of age. Of note ODD-Luc activity was higher in brain and liver as compared to the heart throughout fetal development. At 8 weeks of age (maturity) ODD-Luc activity was ~2-fold higher in the liver as compared to the heart and brain, which were not different in their activities.

3.6. ODD-Luc activity is induced by maternal O_2 deprivation

ODD-Luc activity was robustly induced in the placenta and fetal organs by reduction of maternal inspired O_2 concentration to 8% for 4 hours (room air = 21 % O_2) (Fig. 8A–D). The absolute magnitude of induction was greatest in organs and at developmental stages with the highest basal ODD-Luc activity, in particular the placenta and fetal organs at E9.5 −11.5 of gestation.

3.7. ODD-Luc activity in Hif-1α MATcKO

In order to assess the effect of MATcKO *Hif-1α* on O_2 metabolism in the fetal organs, *Hif-1α*$^{f/f}$,*β-actinCre*$^{+}$ females were mated with ODD-Luc males and treated with TM at E8.5–9.5 as described above. Control mice were of the same mating but the pregnant females were not treated with TM. ODD-Luc activities were measured in placenta and fetal organ tissue lysates at E11.5, 13.5, and 15.5 under basal conditions and after reduction of maternal inspired O_2 concentration to 8% for 4 hours. The values are reported as fold-change relative to CON mice breathing room air. These gestational ages were selected to encompass the large decrease in ODD-Luc activity that occurs due to the maturation of the FPU functioning in O_2 exchange and transport to the fetal tissues. There were no differences in ODD-Luc activities between MATcKO E:Cre^{+} and MATcKO E:Cre^{-} organs on E11.5 and E13.5, and thus these sub-groups were lumped together. As will be described further below, MATcKO E:Cre^{+} embryos were not viable at E15.5 and thus were excluded from this analysis. MATcKO had no effect on basal ODD-Luc activity in the fetal organs at any of the gestational ages examined (Fig. 9A; 21% O_2, CON vs cKO). MATcKO also did not affect the magnitude of hypoxic induction of ODD-Luc activity in E11.5 heart, liver and brain (Fig. 9A; E11.5 CON vs cKO 8% O_2). In contrast, MATcKO rendered the fetuses more

vulnerable to O_2 deprivation at E13.5 and 15.5. At these gestational ages MATcKO synergized with reductions in O_2 concentrations (8% O_2 for 4 hours) to increase ODD-Luc activity in the fetal tissues (Fig. 9A). The induction of ODD-Luc activity caused by MATcKO and O_2 deprivation at later gestational ages is similar to that caused by O_2 deprivation alone at the earlier stage (E11.5) prior to the formation of a functional FPU.

MATcKO increased basal ODD-Luc activity in the E11.5 placenta and this activity was further increased by exposure of the pregnant mouse to the reduced O_2 concentration (8% for 4 hours; Fig. 9B). MATcKO did not increase basal ODD-Luc activity in the E13.5 placenta but synergized with reduction in O_2 concentrations to increase ODD-Luc activity (Fig. 9B). By E15.5 there was no effect of MATcKO on basal or inducible ODD-Luc activity.

3.8. Effect of MATcKO on fetal development

Embryos from MATcKO dams (described in Section 3.1 and Methods) were harvested at E13.5 and E15.5 and analyzed in whole mount and section. MATcKO E:Cre$^-$ embryos were present at the expected Mendelian ratios, were of normal size and wet weight (Table 3), and had normal appearance in whole mount and in H&E stained sections (data not shown). In contrast the MATcKO E:Cre$^+$ embryos, (*Hif-1α* effective heterozygotes cKO) were also normal at E13.5, but by E15.5 were ~12% reduced in crown-rump length and most were non-viable (Table 3). Observed in whole mount these embryos showed severe hemorrhage, edema, and reduction in blood-filled vessels on the surface of the embryo (Fig. 10). In H&E stained sections, the MATcKO E:Cre$^+$ embryos appeared smaller than littermate controls (MATcKO E:Cre$^-$). The hearts of these embryos were delayed in their development. The basic structures and anatomic relationships were normally present, such as the 4-chambered heart, the great vessels (aorta, pulmonary arteries) and their anatomic relationships (Fig. 10 and data not shown). A notable abnormality in the MATcKO E:Cre$^+$ was the marked thickening of the epicardium. There also appeared to be abnormal persistence of mesenchyme in the atrial and ventricular septum. Whether these and other differences represent developmental delay, are secondary to the non-viability that develops between E13.5–15.5, or are specific to the MATcKO synergizing with embryonic effective heterozygosity for *Hif-1α*, will require further study.

4. DISCUSSION

The major observations of this study are that 1) maternal expression of HIF-1α is required within a specific period of gestation for the normal development of the placenta 2) placental defects caused by MATcKO of *Hif-1α* cause placental dysfunction as evidenced by increased susceptibility to hypoxic stress at mid-gestation when the feto-placental unit (FPU) has matured in its function of O_2 transport to the fetal tissues and 3) placental defects caused by MATcKO of *Hif-1α* are exacerbated by fetal heterozygosity of a mutant *Hif-1α* allele and lead to fetal demise later in gestation.

4.1. Hif-1α and placentation

Here we show that Tamoxifen-inducible inactivation of *Hif-1α* specifically in maternal cells at E8.5 of pregnancy causes defects in both the maternal and fetal-derived components of the placenta. When TM is administered at later stages of pregnancy (E10.5) there is no effect (data not shown). These experiments thus establish that HIF-1α is required in the maternal cells between E8.5 and E11.5 in order for placentation to proceed normally. This study did not define a specific mechanism by which HIF-1α in maternal cells is required for placentation. It is well established that in mammals, including humans, the uterine environment and placenta is relatively hypoxic early in development, and that O_2 concentrations increase as the functional feto-placental circulation is established (reviewed in (Burton, 2009; Jauniaux et al., 2003; Murray, 2012). Our measurements of ODD-Luc activity as a surrogate indicator of intra-cellular O_2 concentrations are consistent with this paradigm. A number of roles for hypoxia signaling through HIF have been proposed in the complex orchestration of the many cell types and processes required for normal placentation, a subject not suitably reviewed here (see (Maltepe et al., 2010; Pringle et al., 2010). Studies by Soares and co-workers used hypoxic exposures of pregnant rats, i.e. gain-of-function, to suggest a role for hypoxia/HIF in the recruitment of invasive trophoblasts into the maternal decidua for the purpose of uterine vascular remodeling (Rosario et al., 2008). uNK cells are also thought to be required for the initiation of uterine spiral artery remodeling in humans (Hanna et al., 2006), rats (Chakraborty et al., 2011) and mice (Ashkar et al., 2000; Guimond et al., 1998) (reviewed in (Soares et al., 2014; Tessier et al., 2015). NK cell depletion in the rat delayed spiral artery remodeling and increased Pimonidazole binding and HIF-1α protein in the placenta as markers of placental hypoxia (Chakraborty et al., 2011). In the current study, we observed a reduction in both Prf-positive uNK cells and *Plf* (*Prl2c2*)-positive trophoblast giant cells in the decidua of MATcKO mice. The number of uNK cells was significantly reduced at E13.5 and E15.5 vs CON, while the normal developmental trend of decreasing numbers of uNK cells over this period was unchanged. Maternal HIF-1α could be required for the recruitment, differentiation, proliferation or survival of uNK cells in the decidua. A study by Cerdeira et al. showed that human peripheral NK cells could be induced to acquire the decidual (uterine) NK phenotype by exposure to hypoxia (1% O_2) in vitro. Hypoxia induced secretion of VEGF by uNK cells and reduced NK cytotoxicity, a feature of uNK as compared to peripheral NK cells (Kopcow et al., 2005). In that study, differentiated uNK cells, in turn, promoted migration of the human HTR8/svneo trophoblast cells *in vitro*, a cell line used to model human extravillous trophoblast, which are analogous to mouse *Plf (Prl2c2*)-positive trophoblast giant cells found in the junctional zone and decidua (Cerdeira et al., 2013; Graham et al., 1993; Simmons et al., 2007). Fate mapping studies as described in (Daussy et al., 2014) and (Rosario et al., 2008) will be required to determine the effect of MATcKO *Hif-1α* on uNK and trophoblast giant cells, their potential interdependence and how their roles in remodeling of maternal spiral arteries may be affected by MATcKO.

Our study identified that reduced decidual size, relative to the rest of the placenta, at E13.5 in MATcKO placentas was associated with a reduced number of uNK cells (discussed above), and increase in both junctional zone size and migration of glycogen trophoblast cells to the decidua. The reduction of the uNK population may account for the decreased decidual

size. However, it is interesting to note that the junctional zone and glycogen TB cell migration in the MATcKO placentas at E13.5 are very similar to the E15.5 CON placentas, suggesting that hypoxia/maternal *Hif-1α* controls the maturation of the junctional zone and subsequent glycogen TB cell migration. This theory is supported in a study by Chakraborty et al., that shows that NK cell depletion or maternal exposure to hypoxia causes junctional zone expansion in the rat (Chakraborty et al., 2011). Future studies will be required to investigate this relationship.

The MATcKO placentas, in addition to the altered decidua and junctional zones, have altered labyrinth layers. Independent of fetal genotype, *Gcm1*-positive cells appeared reduced in number and cell size, and ODD-Luc data suggests that MATcKO results in placental hypoxia at E11.5. This is significant because it implicates hypoxia in the control of syncytiotrophoblast differentiation. Supporting this, a study by Chiang et al., showed that hypoxia leads to GCM1 degradation, and that in fact, GCM1 normally autoregulates and promotes its own expression (Chiang et al., 2009). This is of significance to our study as Gcm1 is a key regulator of syncytiotrophoblast differentiation, fusion and branching morphogenesis initiated by trophoblast cells (Anson-Cartwright et al., 2000). Thus, it is possible that the reduction in *Gcm1* expression is caused by placental hypoxia, and in turn, results in the disrupted branching morphogenesis and underdevelopment seen in the labyrinth of MATcKO placentas.

From the current data we cannot distinguish between cell autonomous vs non-autonomous effects of the MATcKO of *Hif-1α* on uNK, trophoblast and other cells of the placenta. This may be addressed through more complete time course experiments, and through the use of cell-type-specific promoters that direct Cre expression, and thus cKO of *Hif-1α*, in specific cell types within the placenta. MATcKO *Hif-1α* could also have adverse effects on the pregnancy, mediated by cells outside of the placenta given that the *α-actin* promoter driving the Tamoxifen-inducible *Cre* is ubiquitously active. However, over the short time course of these experiments MATcKO *Hif-1α* had no effect on maternal hematocrit and the pregnant mice otherwise appeared healthy, suggesting that the effect was placental in origin.

4.2. Placental defects: effects on the fetus

In this and our prior study (Kenchegowda et al., 2014), ODD-Luc was used as a sensitive and quantitative indicator of tissue oxygenation during development. MATcKO of *Hif-1α* and the resultant placental defects did not reduce basal oxygenation of the fetal tissues at E11.5–15.5 as measured by the ODD-Luc reporter. This is important for several reasons. First, it argues against a non-specific effect of the MATcKO. Second, it is consistent with studies of the $Rag2^{-/-}Il2rg^{-/-}$ double KO (alymphoid) mice. The placentas of these dams are abnormal with failure of spiral artery remodeling (Ashkar et al., 2000). Using the semi-quantitative hypoxia indicator pimonidazole, increased fetal or placental tissue hypoxia was not observed in the later stages of development (E18) of these mice, while earlier stages were not examined (Leno-Duran et al., 2010). The current study did observe a significant effect of MATcKO *Hif-1α* and the resulting placental defect on the response to hypoxic stress that was a function of the gestational age. At E11.5 ODD-Luc activity was increased substantially in the fetal organs when the dam's inspired O_2 concentration was reduced to

8%, and there was no further effect of MATcKO. At E13.5 and E15.5, the ODD-Luc activity in the fetal organs had a much smaller increment in response to the lowering of inhaled O_2 concentration. MATcKO *Hif-1α* synergistically increased ODD-Luc activity under hypoxic stress in the fetal organs to the level of the E11.5 fetal organs under hypoxic stress. We interpret these data to indicate that at E11.5 the fetal organs are highly susceptible to O_2 deprivation due to the immaturity of the FPU that functions in O_2 exchange and transport to the tissues. At E13.5–15.5, the FPU is functional. The placental defects generated by MATcKO are not sufficient to disrupt basal O_2 delivery but significantly diminish the O_2 reserve in the system. This model is supported by prior studies that indicate that ~E10.5–13.5 is the stage of mouse development when the embryo/fetus is most susceptible to O_2 deprivation (Kenchegowda et al., 2014; Ream et al., 2008).

Further studies are required to investigate the relationship between timing of MATcKO and effects on placental function and fetal O_2 metabolism. For example, in the current study, the timing of MATcKO *Hif-1α* at E8.5–9.5 is closely coupled to ODD-Luc measurements at E11.5. Would MATcKO, if initiated earlier in gestation, e.g E7.5, cause deficits in O_2 metabolism or reserve at E11.5? Similarly, does MATcKO of *Hif-1α* early in gestation affect ODD-Luc activity as an indicator of O_2 metabolism, or O_2 reserve, in later stages of development? The mother, placenta and fetus may adapt to stressors that reduce O_2 transport, such as increase in cardiac output, O_2 carrying capacity, and placental size, vascularity and surface area for O_2 exchange, to maintain the viability of the fetus (Gassmann et al., 2016; Webster and Abela, 2007; Zhang et al., 2011).

One of the goals of our studies is to understand feto-placental coupling and how placental insufficiency may put the fetus at-risk at critical stages of development. In the current study, embryos that were essentially wild type (*Cre*-) appeared to develop normally when supplied by a structurally abnormal MATcKO placenta. This is consistent with studies of the $Rag2^{-/-}Il2rg^{-/-}$ mouse model of lymphoid (NK cell) deficiency, in which there is defective remodeling of the decidual SAs but minimal effect on fetal development. However, the fetuses and their metabolism were not thoroughly evaluated and adaptations by the mother, placenta and fetus may blunt the adverse effect of this genetic insult present from the time of conception. The current study of induction of a mid-gestational placental defect indicates that fetal O_2 metabolism is normal under basal conditions but more vulnerable to an external stressor such as O_2 deprivation. Therefore, it will be of interest to determine if subjecting the vulnerable MATcKO pregnancy to more prolonged periods of O_2 deprivation during the critical period of organogenesis, or just after, has adverse effects on the E:Cre^- fetus such as growth retardation or structural heart defects. In a different model, in which *Mesp1-Cre* was used to inactivate *Hif-1α* in the mesodermal tissues, exposure to hypoxic stress at E9.5 markedly increased the incidence of congenital heart defects (Oreilly et al., 2014). It was presumed that there was placental insufficiency in this cKO but this was not directly tested.

Embryos that were effectively heterozygous for *Hif-1α* did not develop normally when supplied by a structurally abnormal MATcKO placenta. In contrast, embryos that are germline heterozygous for *Hif-1α* develop normally through adulthood (Kline et al., 2002). Thus, the present study suggests that MATcKO *Hif-1α* induced placental insufficiency has deleterious effects on the development of a genetically at-risk fetus. Stated differently, the

mother provides an environmental stress to the embryo through the defect in hypoxia/HIF-dependent placentation, and passes on genetic risk in a heterozygous state. One caveat to this model is that we cannot exclude an interaction of Cre/TM with the *Hif-1α* heterozygosity in these embryos, though we did not observe an effect in embryos of control Cre^{+}+TM mice. The vulnerability of *Hif-1α* (germline) heterozygous mouse embryos to second stressors has also been observed in a model of maternal diabetes. *Hif-1α* heterozygous null mouse embryos that inherit their *Hif-1α* null allele from their father and are exposed to streptozotocin-induced maternal diabetes during pregnancy have an increased incidence of fetal demise and developmental heart defects compared to their wild-type littermates (Bohuslavova et al., 2013). As placental development has been shown to be affected by maternal diabetes during pregnancy, associated with a several-fold increase in the incidence of congenital heart defects (Øyen et al., 2016), it is a reasonable presumption that in both the Bohuslavova study and in our present study, the fetal *Hif-1α* heterozygous phenotype is exacerbated by maternal-derived placental insufficiency. A number of other germline gene KOs, included in the HIF pathway, cause heart and (often un-recognized) placental defects (reviewed in (Watson and Cross, 2005). In a few of these, such as p38α MAPK and PPAR-γ, the heart defects resolve when the placental defect is rescued by chimeric aggregation (Adams et al., 2000; Barak et al., 1999). In these studies, early cleavage-staged homozygous mutant embryos were aggregated with cleavage-staged 4N tetraploid wild-type embryos, allowed to develop to the blastocyst stage and transferred to pseudo-pregnant dams. In the resulting pregnancies, tetraploid cells contribute exclusively to the trophoblast lineage and therefore make these cells and their subsequent contribution to the placenta, effectively wild-type while the embryo is homozygous null. These findings suggest that the cardiac defects are secondary to placental (trophoblast) dysfunction, though this was not measured in any way. Of note, these and most germline KOs with placental and heart defects cause non-viability at or prior to E11.5. This is still relatively early in placental and heart morphogenesis. Thus, it has not been possible to study the effect of placental dysfunction on the development of a viable fetus in the critical E10.5–13.5 window of mouse organogenesis.

In the current study, we did not define the cause of the growth retardation and demise of these embryos. The thickening of the epicardium could be indicative of a defect in vascularization of the heart, but the phenotypes of non-viable embryos must be interpreted with caution. As with the placenta, fate mapping and time course studies will be of great utility in defining the basis of the cardiac defects. It will be of interest to determine in future studies how MATcKO of *Hif-1α* and resulting placental defects stress and/or disrupt the development of the fetus that is at risk due to additional genetic or environmental stressors.

Acknowledgments

We thank Professor Eugene D. Albrecht and Jeffery S. Babischkin for sharing the histology facility and for assistance with placental tissue processing, and Dr. Jeanine Ursitti for technical assistance.

FUNDING

This work was supported by the Department of Defense (PR140388) and National Institute of Health (R01 HL65314) to S.A.F.

REFERENCES

Adams RH, Porras A, Alonso G, Jones M, Vintersten K, Panelli S, Valladares A, Perez L, Klein R, Nebreda AR. Essential role of p38α MAP kinase in placental but not embryonic cardiovascular development. Mol. Cell. 2000; 6:109–116. [PubMed: 10949032]

Adamson SL, Lu Y, Whiteley KJ, Holmyard D, Hemberger M, Pfarrer C, Cross JC. Interactions between trophoblast cells and the maternal and fetal circulation in the mouse placenta. Dev. Biol. 2002; 250:358–373. [PubMed: 12376109]

Anson-Cartwright L, Dawson K, Holmyard D, Fisher SJ, Lazzarini RA, Cross JC. The glial cells missing-1 protein is essential for branching morphogenesis in the chorioallantoic placenta. Nat. Genet. 2000; 25:311–314. [PubMed: 10888880]

Ashkar AA, Di Santo JP, Croy BA. Interferon gamma contributes to initiation of uterine vascular modification, decidual integrity, and uterine natural killer cell maturation during normal murine pregnancy. J. Exp. Med. 2000; 192:259–270. [PubMed: 10899912]

Auger N, Fraser WD, Healy-Profitós J, Arbour L. Association between preeclampsia and congenital heart defects. J. Am. Med. Assoc. 2015; 314:1588–1598.

Barak Y, Nelson MC, Ong ES, Jones YZ, Ruiz-Lozano P, Chien KR, Koder A, Evans RM. PPAR gamma is required for placental, cardiac, and adipose tissue development. Mol. Cell. 1999; 4:585–595. [PubMed: 10549290]

Bishop T, Ratcliffe PJ. HIF hydroxylase pathways in cardiovascular physiology and medicine. Circ. Res. 2015; 117:65–79. [PubMed: 26089364]

Bohuslavova R, Skvorova L, Sedmera D, Semenza GL, Pavlinkova G. Increased susceptibility of HIF-1α heterozygous-null mice to cardiovascular malformations associated with maternal diabetes. J. Mol. Cell Cardiol. 2013; 60:129–141. [PubMed: 23619295]

Brodwall K, Greve G, Oyen N. Preeclampsia and congenital heart defects. J. Am. Med. Assoc. 2016; 315:1167–1168.

Burton GJ. Oxygen, the Janus gas; its effects on human placental development and function. J. Anat. 2009; 215:27–35. [PubMed: 19175804]

Cerdeira AS, Rajakumar A, Royle CM, Lo A, Husain Z, Thadhani RI, Sukhatme VP, Karumanchi SA, Kopcow HD. Conversion of peripheral blood NK cells to a decidual NK-like phenotype by a cocktail of defined factors. J. Immunol. 2013; 190:3939–3948. [PubMed: 23487420]

Chakraborty D, Rumi MAK, Konno T, Soares MJ. Natural killer cells direct hemochorial placentation by regulating hypoxia-inducible factor dependent trophoblast lineage decisions. Proc. Natl. Acad. Sci. USA. 2011; 108:16295–16300. [PubMed: 21900602]

Chiang MH, Liang FY, Chen CP, Chang CW, Cheong ML, Wang LJ, Liang CY, Lin FY, Chou CC, Chen H. Mechanism of hypoxia-induced GCM1 degradation: implications for the pathogenesis of preeclampsia. J Biol. Chem. 2009; 284:17411–17419. [PubMed: 19416964]

Daussy C, Faure F, Mayol K, Viel S, Gasteiger G, Charrier E, Bienvenu J, Henry T, Debien E, Hasan UA, Marvel J, Yoh K, Takahashi S, Prinz I, de Bernard S, Buffat L, Walzer T. T-bet and Eomes instruct the development of two distinct natural killer cell lineages in the liver and in the bone marrow. J. Exp. Med. 2014; 211:563–577. [PubMed: 24516120]

Dunwoodie SL. The Role of Hypoxia in Development of the Mammalian Embryo. Dev. Cell. 2009; 17:755–773. [PubMed: 20059947]

Fisher SA, Burggren WW. Role of hypoxia in the evolution and development of the cardiovascular system. Antioxid. Redox Signal. 2007; 9:1339–1352. [PubMed: 17627471]

Gassmann NN, van Elteren HA, Goos TG, Morales CR, Rivera M, Martin DS, Cabala Peralta P, Passano del Carpio A, Aranibar Machaca S, Huicho L, Reiss IKM, Gassmann M, de Jonge RCJ. Pregnancy at high altitude in the Andes leads to increased total vessel density in healthy newborns. J. Appl. Physiol. 2016; 121:709–715. [PubMed: 27445300]

Graham CH, Hawley TS, Hawley RG, MacDougall JR, Kerbel RS, Khoo N, Lala PK. Establishment and characterization of first trimester human trophoblast. Exp. Cell Res. 1993; 206:204–211. [PubMed: 7684692]

Guimond MJ, Wang B, Croy BA. Engraftment of bone marrow from severe combined immunodeficient (SCID) mice reverses the reproductive deficits in natural killer cell-deficient tg epsilon 26 mice. J. Exp. Med. 1998; 187:217–223. [PubMed: 9432979]

Hanna J, Goldman-Wohl D, Hamani Y, Avraham I, Greenfield C, Natanson-Yaron S, Prus D, Cohen-Daniel L, Arnon TI, Manaster I, Gazit R, Yutkin V, Benharroch D, Porgador A, Keshet E, Yagel S, Mandelboim O. Decidual NK cells regulate key developmental processes at the human fetal-maternal interface. Nat. Med. 2006; 12:1065–1074. [PubMed: 16892062]

Hayashi S, McMahon AP. Efficient recombination in diverse tissues by a tamoxifen-inducible form of Cre: a tool for temporally regulated gene activation/inactivation in the mouse. Dev. Biol. 2002; 244:305–318. [PubMed: 11944939]

Hemberger M, Nozaki T, Masutani M, Cross JC. Differential expression of angiogenic and vasodilatory factors by invasive trophoblast giant cells depending on depth of invasion. Dev. Dyn. 2003; 227:185–191. [PubMed: 12761846]

Hughes M, Natale BV, Simmons DG, Natale DR. Ly6e expression is restricted to syncytiotrophoblast cells of the mouse placenta. Placenta. 2013; 34:831–835. [PubMed: 23830620]

Jauniaux E, Gulbis B, Burton GJ. Physiological implications of the materno-fetal oxygen gradient in human early pregnancy. Reprod. Biomed. Online. 2003; 7:250–253. [PubMed: 14567901]

Kenchegowda D, Liu H, Thompson K, Luo L, Martin SS, Fisher SA. Vulnerability of the developing heart to oxygen deprivation as a cause of congenital heart defects. J. Am. Heart Assoc. 2014; 3:e000841. [PubMed: 24855117]

Kline DD, Peng YJ, Manalo DJ, Semenza GL, Prabhakar NR. Defective carotid body function and impaired ventilatory responses to chronic hypoxia in mice partially deficient for hypoxia-inducible factor 1α. Proc. Natl. Acad. Sci. USA. 2002; 99:821–826. [PubMed: 11792862]

Kopcow HD, Allan DS, Chen X, Rybalov B, Andzelm MM, Ge B, Strominger JL. Human decidual NK cells form immature activating synapses and are not cytotoxic. Proc. Natl. Acad. Sci. USA. 2005; 102:15563–15568. [PubMed: 16230631]

Leno-Duran E, Hatta K, Bianco J, Yamada AT, Ruiz-Ruiz C, Olivares EG, Croy BA. Fetal-placental hypoxia does not result from failure of spiral arterial modification in mice. Placenta. 2010; 31:731–737. [PubMed: 20580083]

Llurba E, Sanchez O, Ferrer Q, Nicolaides KH, Ruiz A, Dominguez C, Sanchez-de-Toledo J, Garcia-Garcia B, Soro G, Arevalo S, Goya M, Suy A, Perez-Hoyos S, Alijotas-Reig J, Carreras E, Cabero L. Maternal and fetal angiogenic imbalance in congenital heart defects. Eur. Heart J. 2014; 35:701–707. [PubMed: 24159191]

Maltepe E, Bakardjiev AI, Fisher SJ. The placenta: transcriptional, epigenetic, and physiological integration during development. J. Clin. Invest. 2010; 120:1016–1025. [PubMed: 20364099]

Murray AJ. Oxygen delivery and fetal-placental growth: Beyond a question of supply and demand? Placenta. 2012; 33(Suppl. 2):e16–e22. [PubMed: 22742726]

Natale DR, Hemberger M, Hughes M, Cross JC. Activin promotes differentiation of cultured mouse trophoblast stem cells towards a labyrinth cell fate. Dev. Biol. 2009; 335:120–131. [PubMed: 19716815]

Natale DR, Starovic M, Cross JC. Phenotypic analysis of the mouse placenta. Methods Mol. Med. 2006; 121:275–293. [PubMed: 16251749]

Oreilly VC, Floro KL, Shi H, Chapman BE, Preis JI, James AC, Chapman G, Harvey RP, Johnson RS, Grieve SM, Sparrow DB, Dunwoodie SL. Gene-environment interaction demonstrates the vulnerability of the embryonic heart. Dev. Biol. 2014; 18:00140–00147.

Øyen N, Diaz LJ, Leirgul E, Boyd HA, Priest J, Mathiesen ER, Quertermous T, Wohlfahrt J, Melbye M. Prepregnancy diabetes and offspring risk of congenital heart disease: A Nationwide cohort study. Circulation. 2016; 133:2243–2253. [PubMed: 27166384]

Pringle KG, Kind KL, Sferruzzi-Perri AN, Thompson JG, Roberts CT. Beyond oxygen: complex regulation and activity of hypoxia inducible factors in pregnancy. Hum. Reprod. Update. 2010; 16:415–431. [PubMed: 19926662]

Ream M, Ray AM, Chandra R, Chikaraishi DM. Early fetal hypoxia leads to growth restriction and myocardial thinning. Am. J. Physiol. Regul. Integr. Physiol. 2008; 295:R583–R595.

Rosario GX, Konno T, Soares MJ. Maternal hypoxia activates endovascular trophoblast cell invasion. Dev. Biol. 2008; 314:362–375. [PubMed: 18199431]

Ryan HE, Poloni M, McNulty W, Elson D, Gassmann M, Arbeit JM, Johnson RS. Hypoxia-inducible Factor-1α is a positive factor in solid tumor growth. Cancer Res. 2000; 60:4010–4015. [PubMed: 10945599]

Safran M, Kim WY, O'Connell F, Flippin L, Gunzler V, Horner JW, Depinho RA, Kaelin WG Jr. Mouse model for noninvasive imaging of HIF prolyl hydroxylase activity: assessment of an oral agent that stimulates erythropoietin production. Proc. Natl. Acad. Sci. USA. 2006; 103:105–110. [PubMed: 16373502]

Simmons DG, Cross JC. Determinants of trophoblast lineage and cell subtype specification in the mouse placenta. Dev. Biol. 2005; 284:12–24. [PubMed: 15963972]

Simmons DG, Fortier AL, Cross JC. Diverse subtypes and developmental origins of trophoblast giant cells in the mouse placenta. Dev. Biol. 2007; 304:567–578. [PubMed: 17289015]

Simmons DG, Natale DR, Begay V, Hughes M, Leutz A, Cross JC. Early patterning of the chorion leads to the trilaminar trophoblast cell structure in the placental labyrinth. Development. 2008a; 135:2083–2091. [PubMed: 18448564]

Simmons DG, Rawn S, Davies A, Hughes M, Cross JC. Spatial and temporal expression of the 23 murine Prolactin/Placental Lactogen-related genes is not associated with their position in the locus. BMC Genomics. 2008b; 9:352. [PubMed: 18662396]

Sliwa K, Mebazaa A. Possible joint pathways of early pre-eclampsia and congenital heart defects via angiogenic imbalance and potential evidence for cardio-placental syndrome. Eur. Heart J. 2014; 35:680–682. [PubMed: 24302271]

Soares MJ, Chakraborty D, Kubota K, Renaud SJ, Rumi MA. Adaptive mechanisms controlling uterine spiral artery remodeling during the establishment of pregnancy. Int. J. Dev. Biol. 2014; 58:247–259. [PubMed: 25023691]

Tessier DR, Yockell-Lelievre J, Gruslin A. Uterine spiral artery remodeling: The role of uterine natural killer cells and extravillous trophoblasts in normal and high-risk human pregnancies. Am. J. Reprod. Immunol. 2015; 74:1–11. [PubMed: 25472023]

Watson ED, Cross JC. Development of structures and transport functions in the mouse placenta. Physiology. 2005; 20:180–193. [PubMed: 15888575]

Webster WS, Abela D. The effect of hypoxia in development. Birth Defects Res. C Embryo Today. 2007; 81:215–228. [PubMed: 17963271]

Zhang J, Adams MA, Croy BA. Alterations in maternal and fetal heart functions accompany failed spiral arterial remodeling in pregnant mice. Am. J. Obstet. Gynecol. 2011; 205:485. e1–485.e16.

Highlights

- Inactivation of HIF-1α in the mother causes placental defects
- May be due to failed recruitment of trophoblast and natural killer cells to decidua
- Placental defects compromise O_2 delivery to the fetus during hypoxic challenge
- Effects are specific to gestational age
- Supports role for O_2/HIF in disorders of early pregnancy

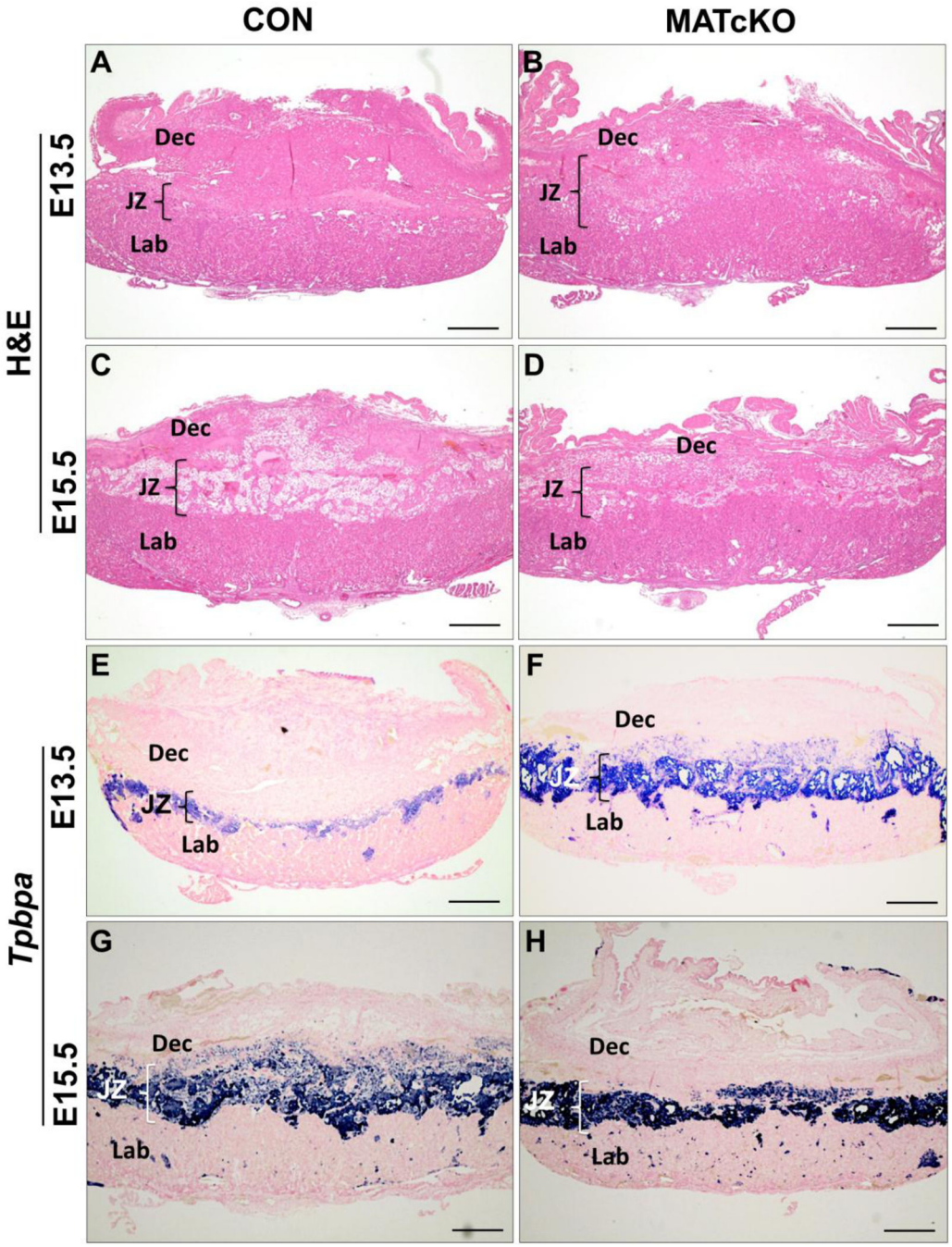

Figure 1.

Conditional knock-out of *Hif-1*α in maternal cells (MATcKO) causes placental defects. *Hif-α*$^{f/f}$, β-*actinCre*$^{+}$ females were mated with wild type males and injected with Tamoxifen (3 mg/40 g bw) on E8.5 and 9.5. Control (CON) pregnant mice were β-*actinCre*$^{+}$ and treated with Tamoxifen in the same manner. Placentas were harvested at E13.5 and E15.5, sectioned in a sagittal plane, and histological assays performed as described in Methods. A-D show H&E stained sections of CON and MATcKO placentas at E13.5 and E15.5. While the overall structure is preserved in MATcKO (B) when compared to CON (A) at E13.5, the

relative thickness of the decidual layer was decreased and the junctional zone increased as a proportion of total placental area. At E15.5, the MATcKO (D) placental thickness increased as a proportion of total placental area while the junctional zone thickness remained unchanged. E-H) I*n situ* hybridization was performed to detect *Tpbpa*, a marker of spongiotrophoblasts, and samples were counterstained with nuclear fast red. An increase of *Tpbpa* staining in the junctional zone of MATcKO placentas is observed at E13.5 as compared to CON (E, F). By E15.5, *Tpbpa* staining in CON placentas increased and appears similar to MATcKO (G, H). Dec- Decidua, JZ- Junctional Zone, Lab- Labyrinth; Tpbpa- Trophoblast specific protein α, Scale bars (μm): A-H, 500.

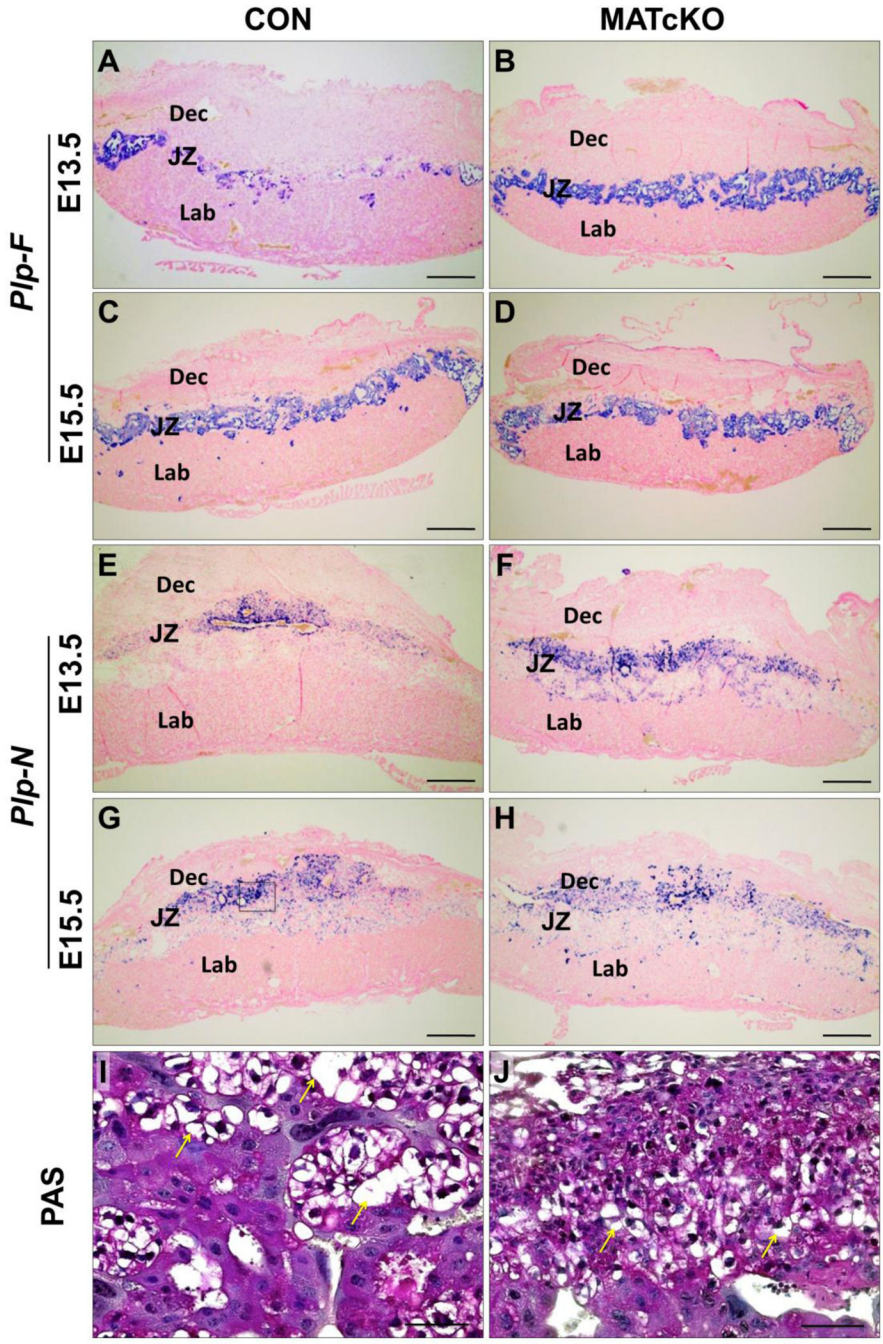

Figure 2.

MATcKO *Hif-1α* affects differentiation of spongiotrophoblast and glycogen trophoblast cells. E13.5 and E15.5 sections from CON (A, C, G, I) and MATcKO (B, D, F, H, J) placentas were examined by in situ hybridization for *Plp-F* to identify spongiotrophoblasts (A–D). *Plp-N* (E–H) and PAS (I, J) were used to identify glycogen trophoblasts. Staining of both *Plp-F* and *Plp-N* was increased in E13.5 MATcKO as compared to CON, while staining for both genes was similar at E15.5 in CON and MATcKO. However, assessment of glycogen trophoblast morphology by PAS staining at E15.5 in CON (I) versus MATcKO (J)

placentas indicated smaller, more compact morphology in MATcKO. The box in G indicates a representative area of junctional zone as shown in I and J. Yellow arrows indicate glycogen trophoblasts. Scale bars (μm): AH: 500; I, J: 50.

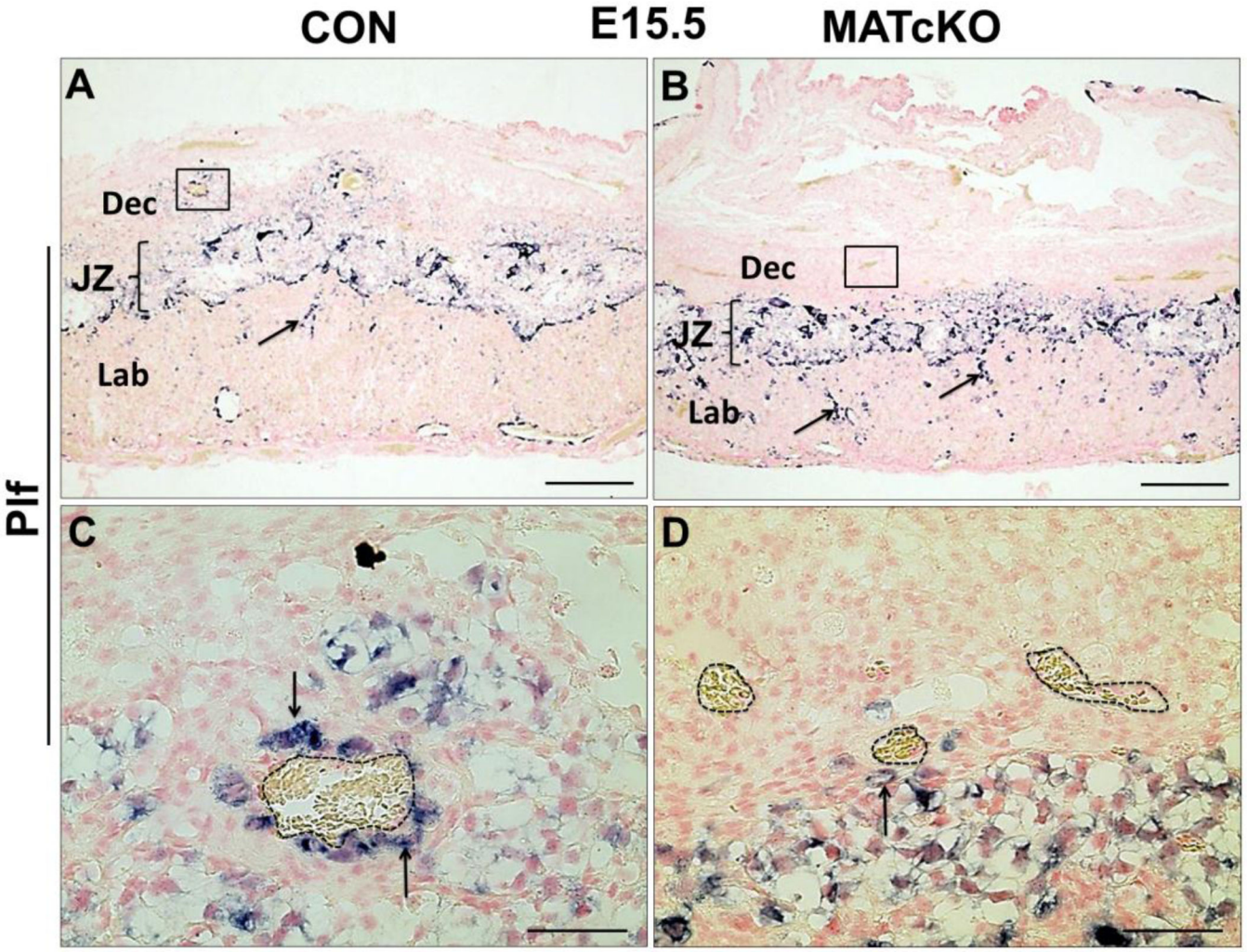

Figure 3.

MATcKO *Hif-1α* affects trophoblast giant cells. Sections from E15.5 CON and MATcKO placentas were examined by *in situ* hybridization for *Plf* (*Prl2c2*). *Plf* (*Prl2c2*)-expressing spiral artery-associated trophoblast giant cells (SpA-TGCs) are present in the junctional zone and decidua of CON placenta (A) and in the junctional zone of MATcKO, but are substantially reduced in the decidua of MATcKO (B). There are increased numbers of *Plf (Prl2c2*) positive cells in the labyrinth of MATcKO placenta (B, arrows). The boxed areas in A and B are shown at higher magnification in C and D where the Plf (*Prl2c2*) positive cells can be seen surrounding the spiral arterioles in the decidua of CON (C, arrows) but not in MATcKO (D). Dotted lines in C and D indicate maternal arterioles. Scale bars (μm): A, B: 500; C, D: 50.

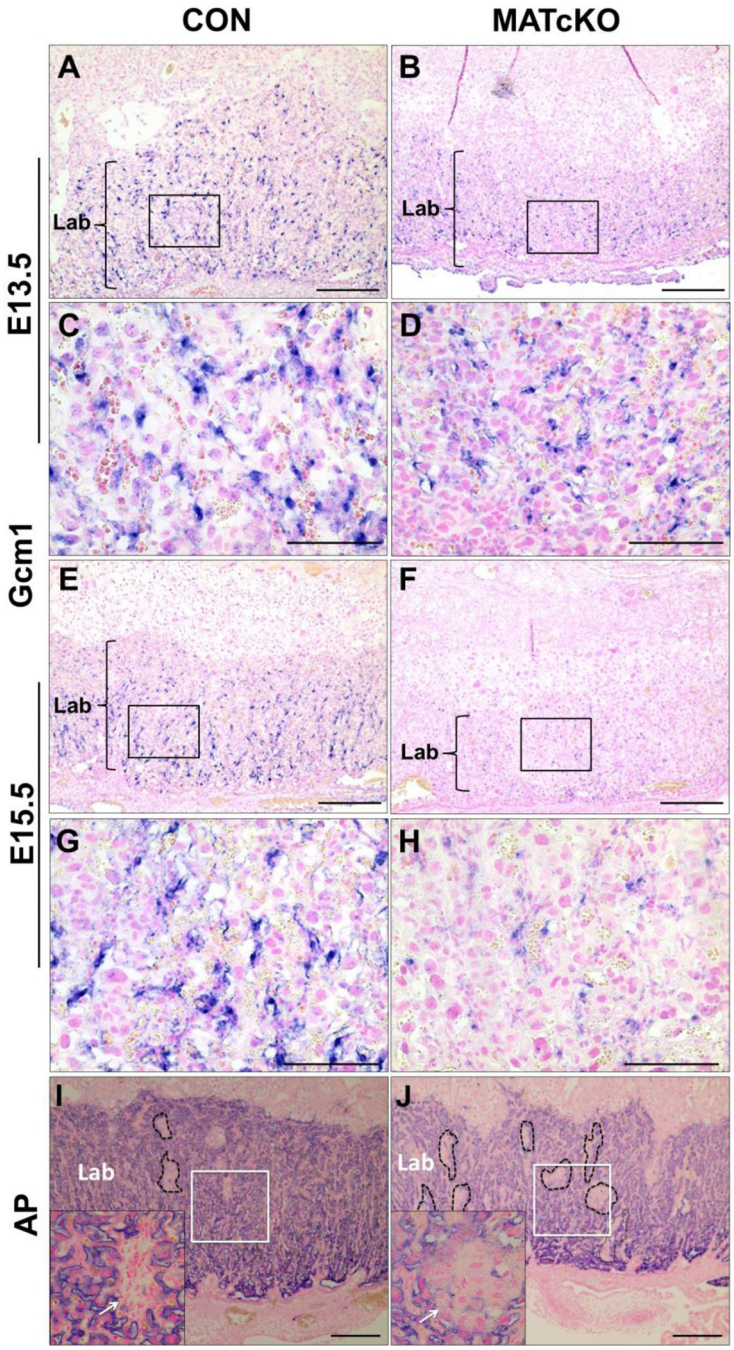

Figure 4.

MATcKO *Hif-1α* decreases expression of *Gcm1*, a marker of syncytiotrophoblast differentiation, and alters labyrinth morphology. Sections from E13.5 (A–D) and E15.5 (E–H) CON and MATcKO E:Cre+ placentas were examined by *in situ* hybridization with a probe against *Gcm1* and at E15.5 by alkaline phosphatase (AP) staining (I, J) to identify maternal blood spaces in the labyrinth. *Gcm1* appears decreased in the labyrinth of the MATcKO (B, D, F, H) compared to CON placentas (A, C, E, G). Higher magnification of boxed areas in A, B, E, F are shown in C, D, G, H. Alkaline Phosphatase (AP) staining in

MATcKO E:Cre+ (J) is notable for increased number of avascular spaces (dotted lines and arrows) as compared to CON (I). Shown as insets are high magnification images of the boxed areas. Arrows in insets, avascular spaces; Lab- Labyrinth; *Gcm1*, glial cells missing homolog 1. Scale bars (μm): A, B, E, F: 500; C, D, G, H: 50; I, J: 300.

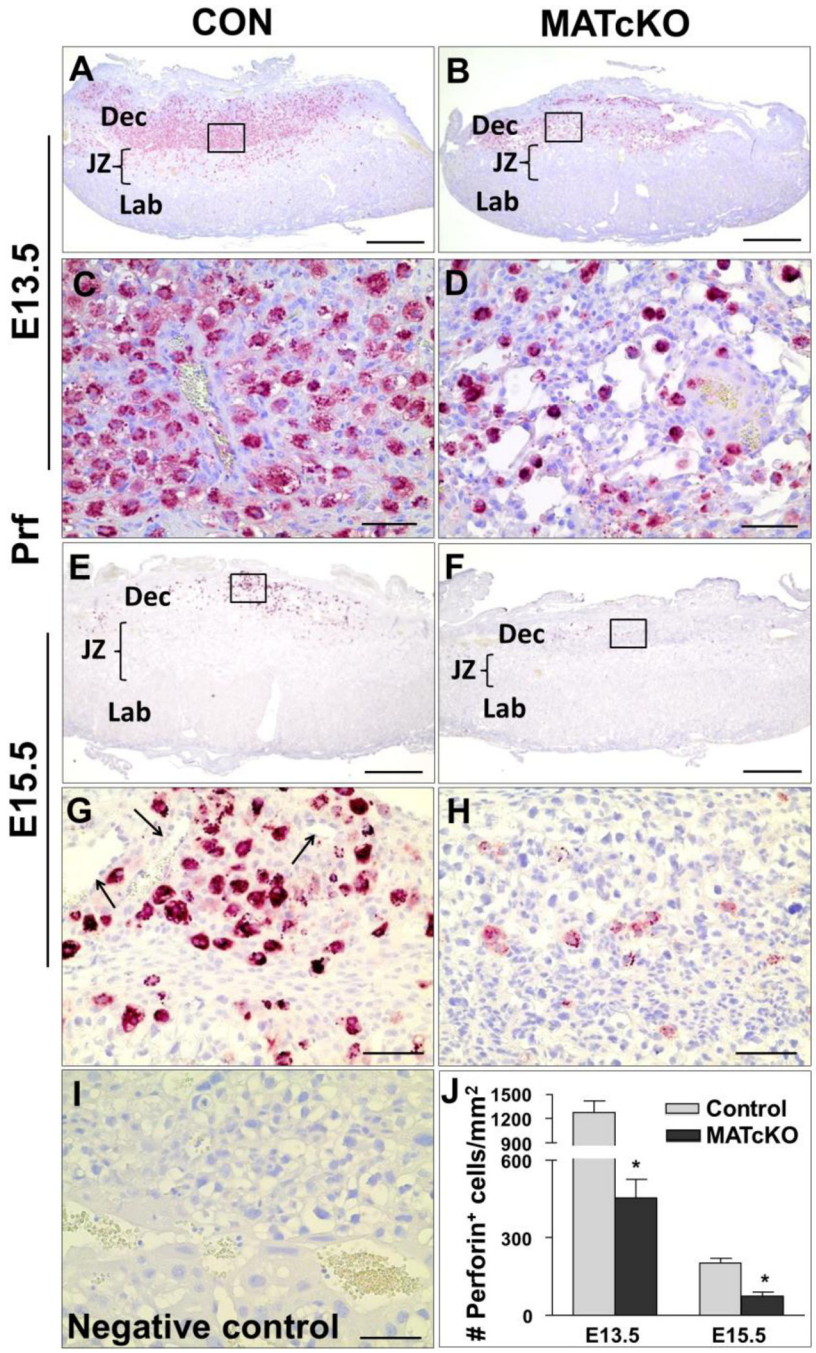

Figure 5.

MATcKO *Hif-1α* causes reduction in uterine Natural Killer (uNK) cells in the placental decidua. Maternally derived uNK cells were detected by immunostaining of E13.5 and E15.5 placentas using anti-Perforin antibody as described in Methods. The number of Perforin positive cells are significantly decreased at E13.5 and E15.5 in the decidua of MATcKO (B, F) as compared to CON (A, E). The boxed areas in A, B and E, F are shown at higher magnification in C, D and G, H respectively. Arrows in (G) indicate maternal decidual arterioles. J) The number of perforin positive cells were counted in 2–3 fields of

view per section and presented as number (#) of perforin positive cells/mm^2. I) No primary antibody (negative control). Values are mean ± SEM *$p<0.001$, n=4–6. Scale bars (μm): A, B, E, F: 500; C, D, G – I: 50.

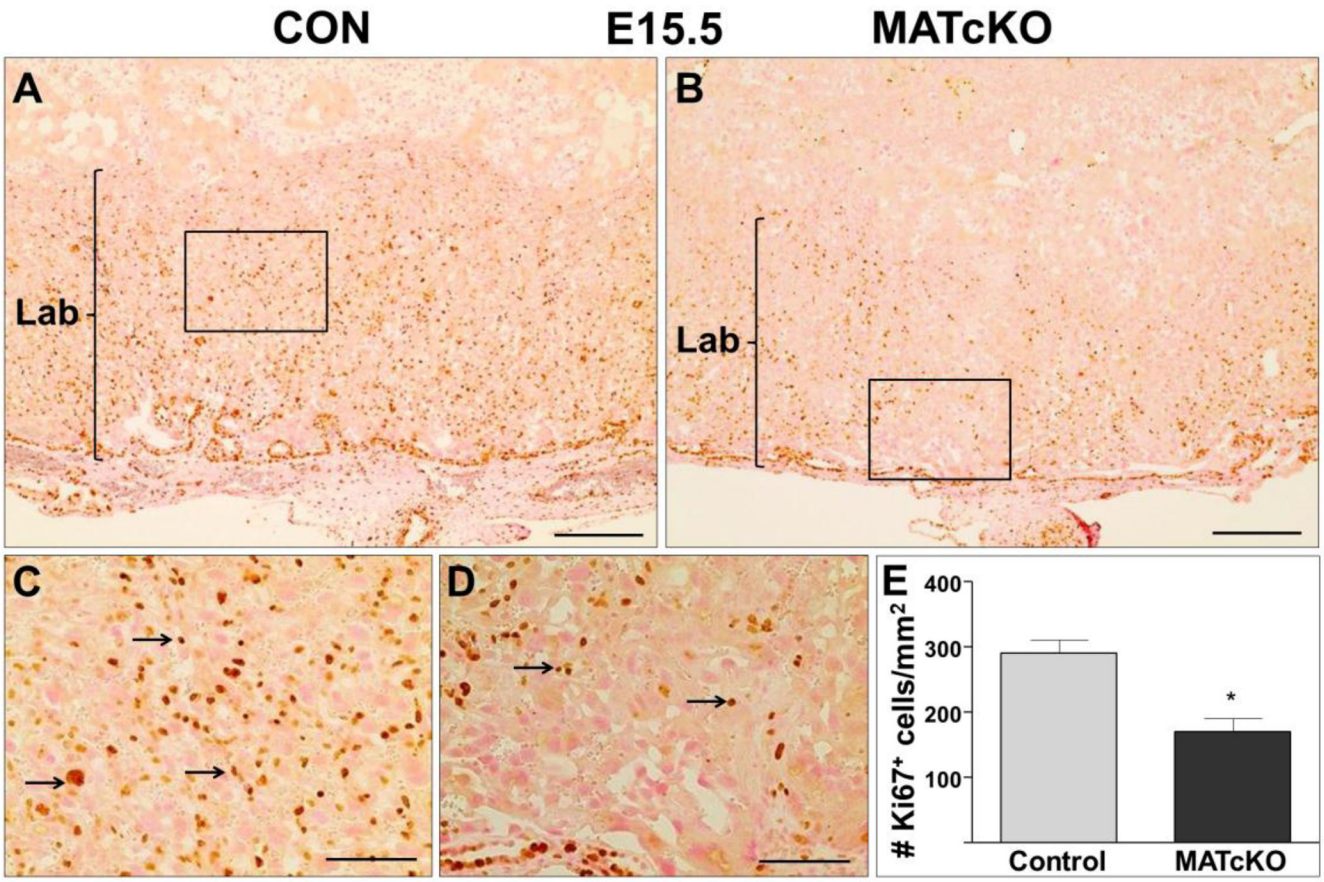

Figure 6.

MATcKO *Hif-1α* reduced the number of Ki67 positive cells in E15.5 placental labyrinth. Ki67 was detected by immuno-staining as described in Methods and used as an indicator of cell proliferation. The number of Ki67 positive cells are significantly decreased in the labyrinth of E15.5 MATcKO placentas (B) as compared to CON (A). The boxed areas in A, B are shown at higher magnification in C, D. Arrows in (C, D) indicate Ki67 positive cells. E) The number of Ki67 positive cells in the labyrinth were counted in one field of view per section and presented as number of Ki67 positive cells/mm^2 Values are mean ± SEM, *$p<0.05$, n=6 Scale bars (μm): A, B: 300; C, D: 100.

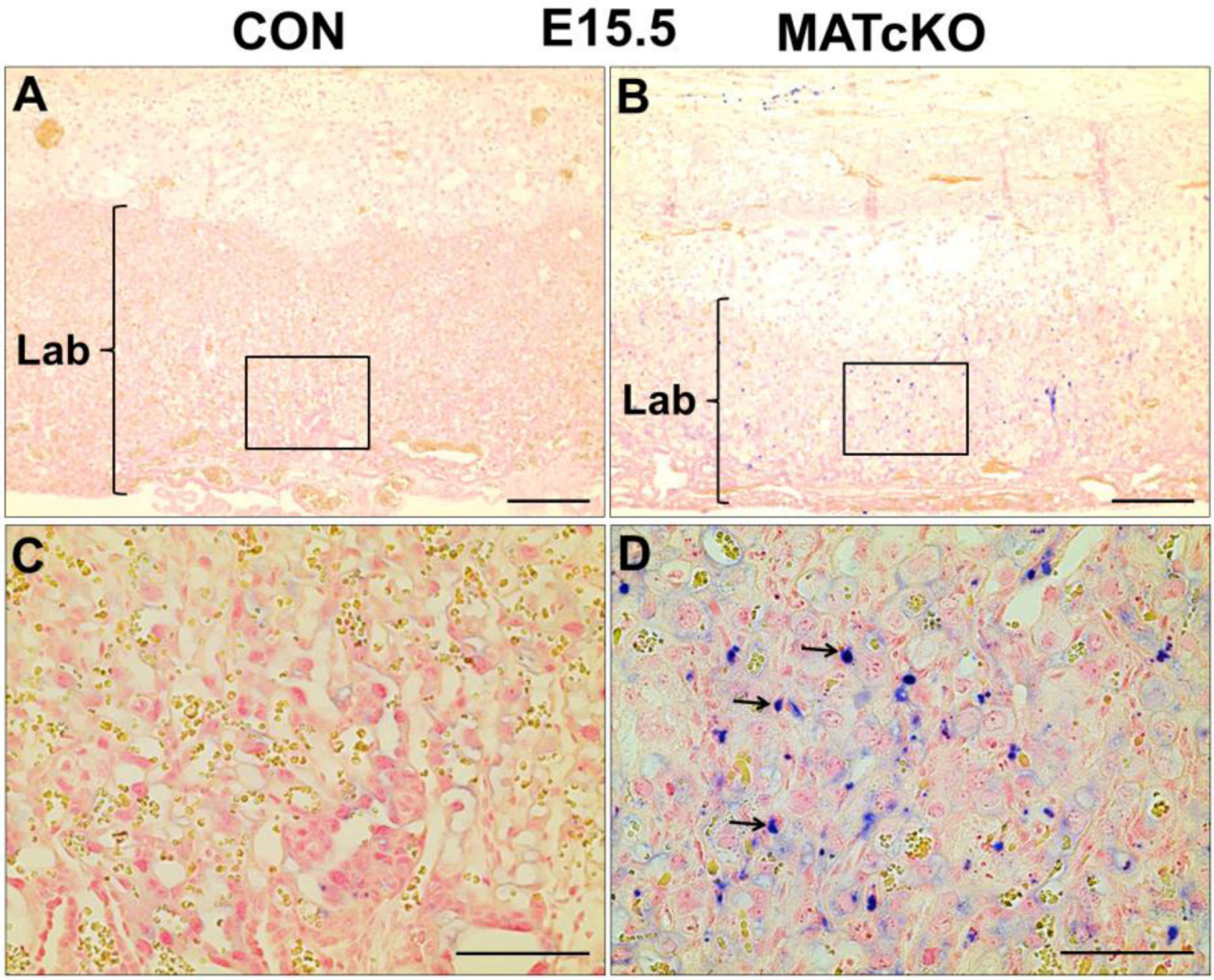

Figure 7.

MATcKO *Hif-1α* induced TUNEL positive cells in E15.5 placental labyrinth. Apoptosis was detected by the TUNEL assay which identified DNA fragmentation in E15.5 placentas. TUNEL positive cells are present in the labyrinth of MATcKO placentas (B) and not in CON (A). The boxed areas in A, B are shown at higher magnification in C, D. Arrows in (D) indicate TUNEL positive cells. Scale bars (μm): A, B: 300; C, D: 100.

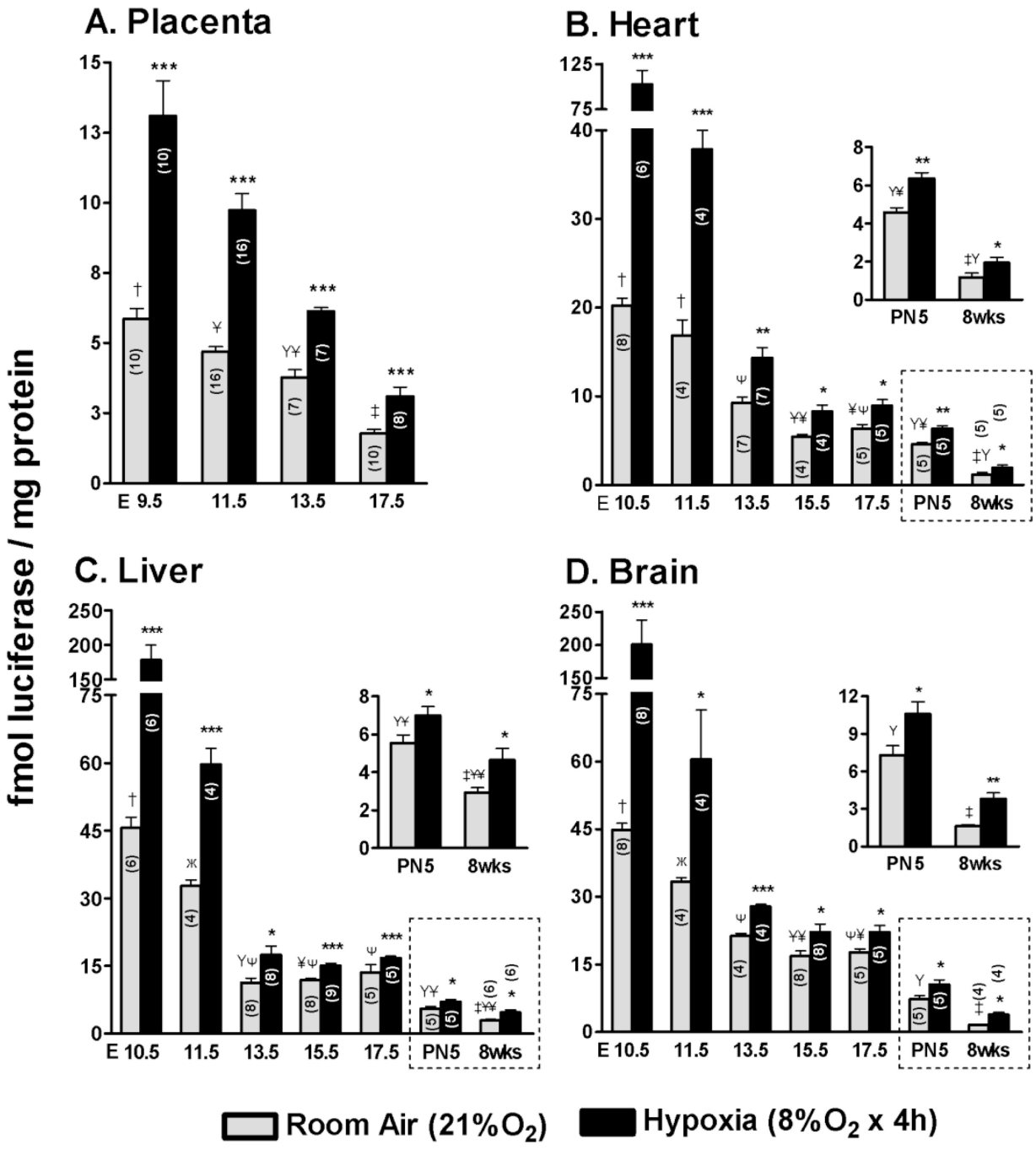

Figure 8.

ODD-Luc activity declines during normal mouse development and is robustly induced by maternal O_2 deprivation in proportion to the basal levels. Mice were homozygous for ODD-Luc (Oxygen Degradation Domain of *Hif-1α* fused to Luciferase reporter protein) expressed from the *ROSA* locus. ODD-Luc mice underwent timed breedings and organs were harvested at the indicated days of gestation. Luciferase activity was measured in lysates from A) placenta B) heart C) liver and D) brain from E9.5- or 10.5 −17.5, at post-natal day 5 (PN5) and maturity (8 weeks). Pregnant ODD-Luc mice from the same stages were

subjected to reduced concentrations of inspired oxygen (8% O_2 for 4 hours) and luciferase activity was measured. Luciferase activity was normalized to total protein and expressed as fmol Luciferase/mg protein. Data in dotted boxes in B, C, D are re-shown in insets with a compressed y-axis for clarity. The number of samples in each group is indicated within the bar graph (n). Student's *t*- test was used for comparison of hypoxia vs. room air samples. **P*<0.05; ***P*<0.01; ****P*<0.001. In the developmental series shown in A, B, C and D, basal luciferase activity (Room air) was analyzed by one-way ANOVA with Bonferroni correction for multiple comparisons; groups sharing the same symbol are not significantly different (*P*>0.05).

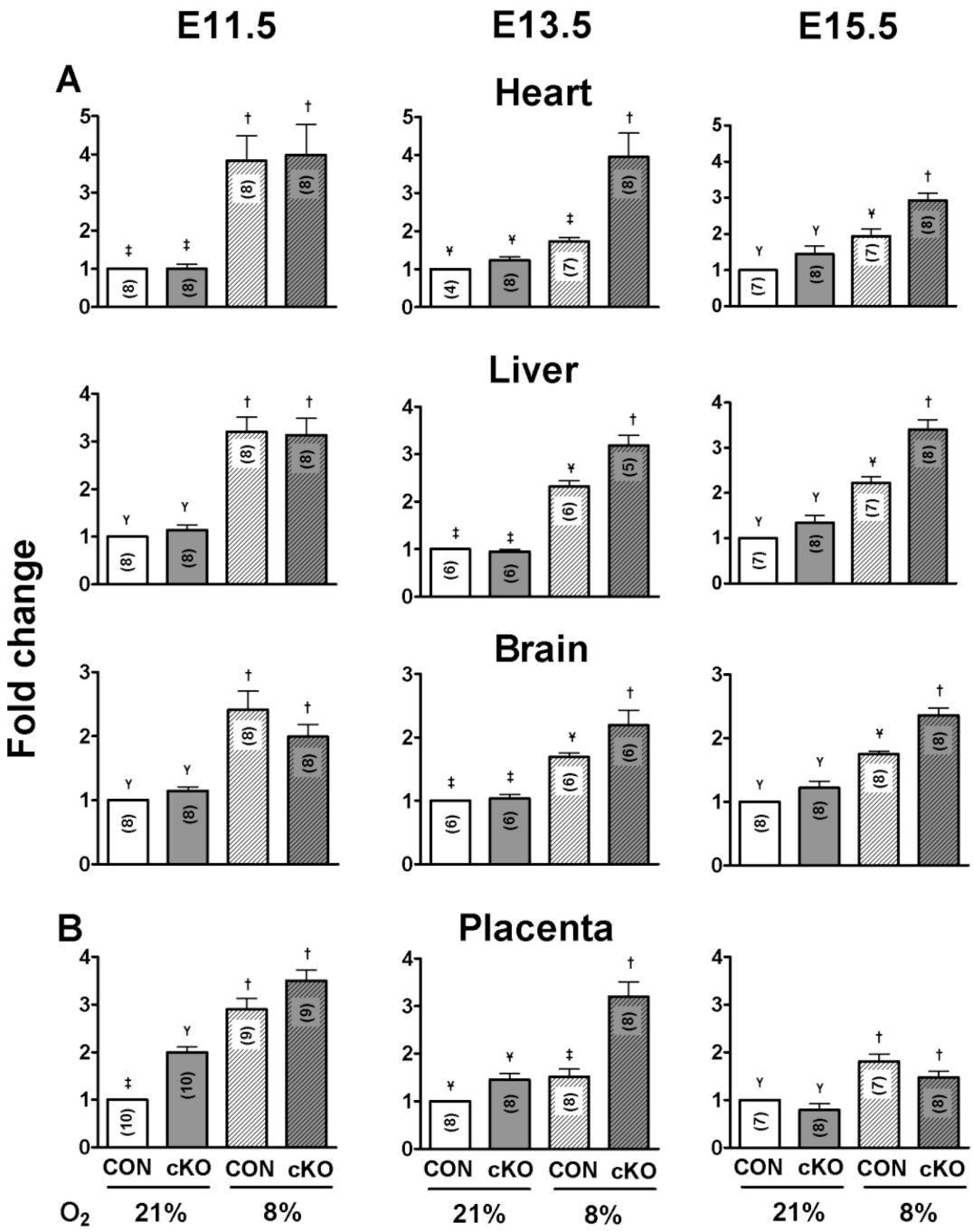

Figure 9.

Conditional knock-out of *Hif-1α* in maternal cells reduces O_2 reserve at E13.5. *Hif-1α*$^{f/f}$*β-actinCre*$^{+}$ females were mated with ODD-Luc homozygous males and injected with Tamoxifen (3 mg/40 g bw) on E8.5 and 9.5. Control mice (*β-actinCre*$^{+}$) were mated with ODD-Luc males and treated with Tamoxifen in the same manner. One-half of the pregnant mice in each group were subjected to reduced concentrations of inspired O_2 (8% O_2 for 4 hours) at E11.5 or E13.5 or E15.5 and then euthanized. ODD-Luc activity per mg protein was measured in the placenta and fetal organs as described above. ODD-Luc activity in each

organ at the gestational ages indicated was normalized to the value from the control mice under room air (21% O_2) and reported as fold-change. The number of samples in each group is indicated within the bar graph (n). Values in the different groups were compared by one-way ANOVA with Bonferroni correction for multiple comparisons; groups sharing the same symbol are not significantly different ($P>0.05$).

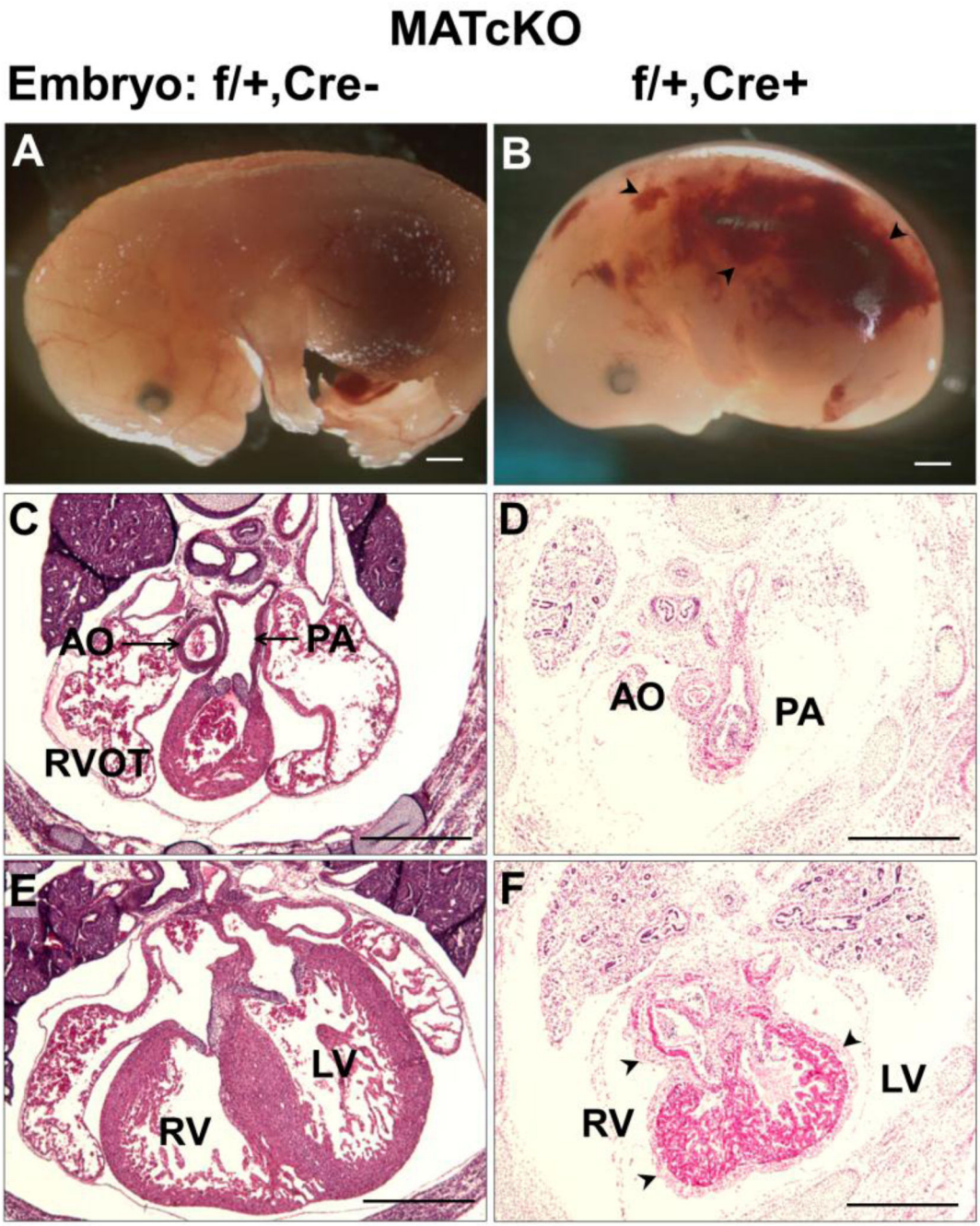

Figure 10.

MATcKO *Hif-1a* results in fetal defects in *Hif-1a* heterozygous null embryos (*Hif-1a*$^{f/+}$,Cre^{+}). MATcKO *Hif-1a* was achieved as described in Fig. 1. Shown are embryos from a MATcKO dam that are effectively WT (*Hif-1a*$^{f/+}$,Cre) (A,C,E) versus *Hif-1a* heterozygous null (B,D,F). Embryos are shown in whole mount (A, B) and in H&E stained sections (C–F) from anterior to posterior with respect to the heart. The WT embryos have normal appearance in whole mount (A) and in sections (C, E). The *Hif-1a heterozygous null* embryos are smaller and edematous and can be seen to have hemorrhages (arrow heads in

B). Embryos of this genotype were non-viable at E15.5. D, F) *Hif-1α* heterozygous null hearts were smaller, showed thickened epicardium (arrow head) and increased mesenchymal tissue in the septum. AO, Aorta; PA, Pulmonary artery; RVOT, Right ventricular outflow tract; RV, Right ventricle, LV, Left ventricle. Scale bars (mm): A, B: 1.0; C-F: 0.5.

Table 1

Placenta morphology assessment; layers as a proportion of total placental area

ED	Groups	Embryo Genotype		Decidua (%)	Junctional zone (%)	Labyrinth (%)
		HIF-1α	Cre			
13.5	CON	+/+	+ and −	48.7±4.0	12.8±1.2	38.4±4.4
	MATcKO	f/+	−	34.2±3.0 *	22.7±0.3 **	43.0±3.2
		f/+	+	35.6±1.3 *	21.8±2.0 *	42.6±2.5
15.5	CON	+/+	+ and −	25.2±0.0	24.4±1.4	50.4±1.4
	MATcKO	f/+	−	26.6±2.4	22.5±0.6	51.0±2.0
		f/+	+	32.2±2.1 *	24.3±2.3	43.4±4.3

Values are mean ± SEM; n= 3–5 placentas in each group;

* P<0.05;

** P<0.001.

Table 2

Effect of maternal and fetal genotype on the expression of markers of trophoblast cells in the placenta

ED	Groups	Embryo Genotype		% Plpn^{+}	% Plpf^{+}	% Tpbpa
		HIF-1α	Cre			
13.5	CON	+/+	+ and −	2.5±0.6	5.3±2.2	10.1±1.6
	MATcKO	f/+	−	14.1±1.5**	11.0±1.0*	22.9±1.9**
		f/+	+	10.3±1.0**	12.2±0.4**	22.5±1.1**
15.5	CON	+/+	+ and −	10.2±1.0	11.6±0.8	25.6±1.1
	MATcKO	f/+	−	11.8±0.6	12.3±1.0	24.7±1.4
		f/+	+	12.6±2.1	12.9±1.3	26.0±1.4

Values are mean ± SEM; n= 3–5 placentas in each group;

*P<0.05;

**P<0.01.

Table 3

Effect of MATcKO on fetal viability, weights and crown-rump length

ED	Groups	# dams	Embryo Genotype		# embryos	# viable	% Non-viable	Fetal Weight (mg)	Crown rump (mm)
			HIF-1α	Cre					
13.5	CON	6	+/+	+ and −	33	33	0	167±20	10.1±0.6
	MATcKO	6	f/+	−	25	25	0	164±10	9.8±0.7
			f/+	+	31	30	3	158±13	10.2±0.5
15.5	CON	5	+/+	+	30	30	0	506±47	15.0±1.0
	MATcKO	7	f/+	−	31	31	0	517±83	15.8±0.8
			f/+	+	28	1	96	477±95	13.9±0.6 *

Fetal weights and crown-rump lengths are mean ± SEM;

* $p<0.05$.